Low-loss photonic integrated circuits for UV applications

W. A. P. Hendriks, M. Dijkstra, S. Mardani, I. Hegeman, Sonia Garcia-Blanco

W. A. P. M. Hendriks, M. Dijkstra, S. Mardani, I. Hegeman, Sonia M. Garcia-Blanco, "Low-loss photonic integrated circuits for UV applications," Proc. SPIE 12424, Integrated Optics: Devices, Materials, and Technologies XXVII, 1242402 (17 March 2023); doi: 10.1117/12.2657143

SPIE.

Event: SPIE OPTO, 2023, San Francisco, California, United States

Low-loss photonic integrated circuits for UV applications

W.A.P.M. Hendriks, M. Dijkstra, S. Mardani, I. Hegeman, Sonia M. Garcia-Blanco
Integrated Optical Systems Group, MESA+ Institute, University of Twente, P.O. Box 217, 7550 AE, Enschede, The Netherlands

ABSTRACT

We present a low propagation loss aluminium oxide integrated photonics platform enabling applications with operation down to the UV wavelength range (i.e., <250 nm). Single mode fully etched waveguides were fabricated with losses below 2 dB/cm at 405 nm. The influence of waveguide dimensions on the propagation losses are presented, indicating that losses are sidewall roughness limited. Lower losses can be achieved by further optimization of the cross-section of the waveguides. In this presentation, the aluminium oxide platform will be introduced together with the characterization of the waveguides at near-UV wavelengths.

Keywords: Aluminium oxide, refractive index, low loss, ultraviolet, UV, PIC

1. INTRODUCTION

Silicon photonics has enabled huge developments in fields including signal processing *[1]*, nonlinear optics *[2]* and quantum information processing *[3]*. Amongst the different silicon photonic platforms, silicon nitride based devices are quite mature, particularly for visible and near infrared (NIR) wavelengths *[4], [5]*. Although excellent demonstrations of low-loss waveguiding in low contrast Si_3N_4 waveguides down to 405 nm *[6]*, injection locked lasers at 410 nm [7] and 404 nm *[8]* have been recently published, the bandgap of Si_3N_4 limits its utilization at UV wavelengths. A need for low-loss photonic integrated circuits (PICs) in the UV exists, to enable applications such as quantum ion traps *[9]*, atomic clocks *[10]* and spectroscopy. Aluminium oxide (Al_2O_3) possesses a bandgap between 5.1 and 7.6 eV depending on the fabrication method*[11]*, facilitating devices down to 250 nm. In addition, an moderate refractive index contrast with silicon dioxide (SiO_2) leads to reduced scattering losses from roughness while the minimum device features are still reasonable as they scale with the wavelength. Al_2O_3 waveguides deposited by atomic layer deposition (ALD) and cladded with SiO_2 have shown losses down to 1.8 dB/cm at 405 nm *[12]*. With air cladding, losses as low as 3 dB/cm have been reached at 370 nm *[13]*. These losses demonstrate the feasibility for Al_2O_3 PICs in the UV. ALD is however a slow *[14]* and relatively expensive process. In this paper, we present a low-loss reactive sputtered Al_2O_3 UV PIC platform. First, the waveguide design is discussed ensuring single mode operation. Next, slab losses in the UV of the deposited layers are discussed. Finally, channel propagation losses measured at 405 nm using a cutback method are presented.

2. DESIGN

Single transverse mode operation is a prerequisite for most PIC components. We have therefore chosen the investigated waveguide dimensions to support single mode operation. We choose to fix the layer thickness at 70 nm as this is the minimum thickness that still supports mode propagation at 377 nm, thereby allowing for quality control of the layer after deposition. For quality control, the layer propagation losses are measured using a Metricon M2010 prism coupling setup. For the results presented here the losses after deposition where found to be 0.7 dB/cm at 377 nm. To determine suitable waveguide widths for 405 nm light, finite difference eigenmode simulations are performed to determine the refractive index as a function of waveguide width. The results shown in *Figure 1* indicate that a higher order mode starts at a width of 670 nm. For this reason we choose a maximum waveguide width of 700 nm as the higher order TE mode is not supported when even a slight bend is applied. The minimum waveguide width is chosen at 400 nm as this still exhibits negligible bend losses at a bend radius of 500 µm.

Integrated Optics: Devices, Materials, and Technologies XXVII, edited by Sonia M. García-Blanco, Pavel Cheben, Proc. of SPIE Vol. 12424, 1242402 · © 2023 SPIE
0277-786X · doi: 10.1117/12.2657143

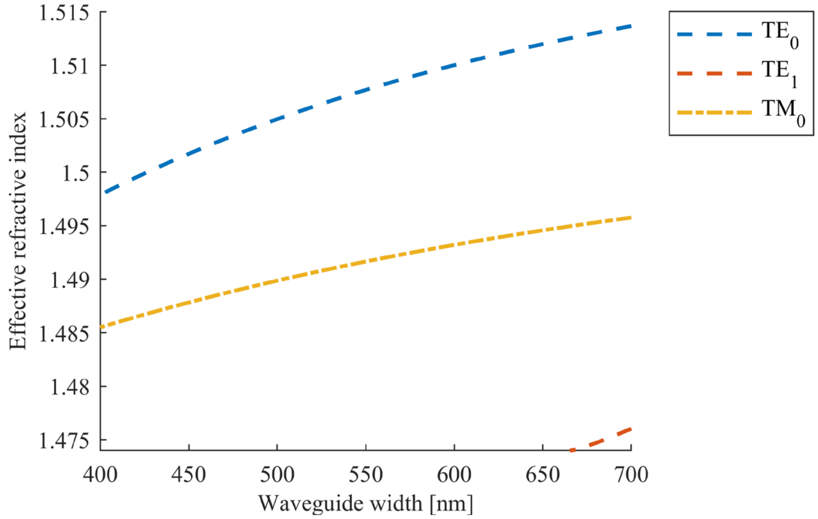

Figure 1 Effective index of an 70 nm high Al_2O_3 waveguide as a function of its width for light at 405 nm.

3. RESULTS

We demonstrate the suitability of the Al_2O_3 waveguides for UV applications by UV-Vis transmission measurements as well as channel waveguide loss measurements using a cutback method at 405 nm. The UV-Vis transmission measurement is performed on a quartz substrate coated with an ~850 nm layer of Al_2O_3 using a quartz substrate as reference. The resulting transmission loss as presented in *Figure 2* shows that the absorption of the Al_2O_3 layer starts to markedly increase from <250 nm demonstrating the feasibility for waveguide operation below 250 nm.

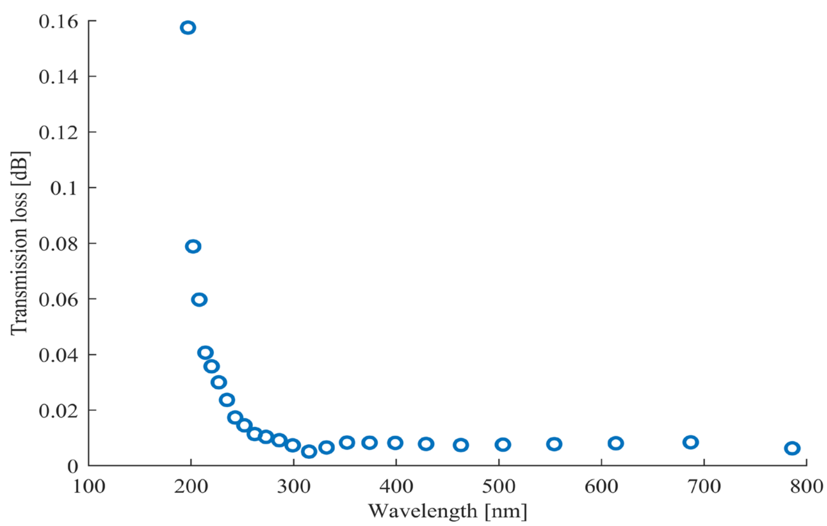

Figure 2 Transmission loss spectrum of sputter coated Al_2O_3. The observed dip at 310 nm is caused by the switching between the halogen and deuterium lamp.

The PICs for the waveguide loss measurements are fabricated by electron beam lithography. They consist of a circuit with spirals of varying propagation lengths from 3.3 to 14 cm. After development, the waveguides pattern is transferred into the Al_2O_3 using reactive ion etching. Next, a SiO_2 cladding is deposited and the circuits are diced. For the cutback measurements light from a polarization maintaining (PM) fiber-coupled 405 nm laser source is butt-coupled to the chip using pm-s350-hp fibers. Although taper couplers are implemented in the circuits, high coupling losses in excess of

30 dB per facet are observed. We expect the facet roughness to be a major contributor to these losses, as the end facets are not polished. In addition, bend losses can be observed in the camera image taken from the propagation through the waveguide in *Figure 3*.

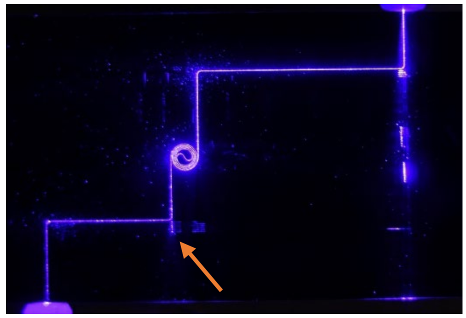

Figure 3 Top view of 405 nm light coupled into an Al_2O_3 PIC. The arrow indicates light lost at the bend scattering from waveguides that are routed perpendicular.

To determine the propagation losses, the power transmitted (in dB) as a function of channel length is plotted and an linear fit is used to determine the propagation losses. The results for the given waveguide widths for both TE and TM polarization are shown in *Figure 4*. We observe a clear loss reduction when the waveguide width is increased from 400 to 500 nm, indicating a significant sidewall roughness contribution to the losses. Observed losses for the consecutive widths have clearly overlapping confidence intervals making any further conclusion precarious.

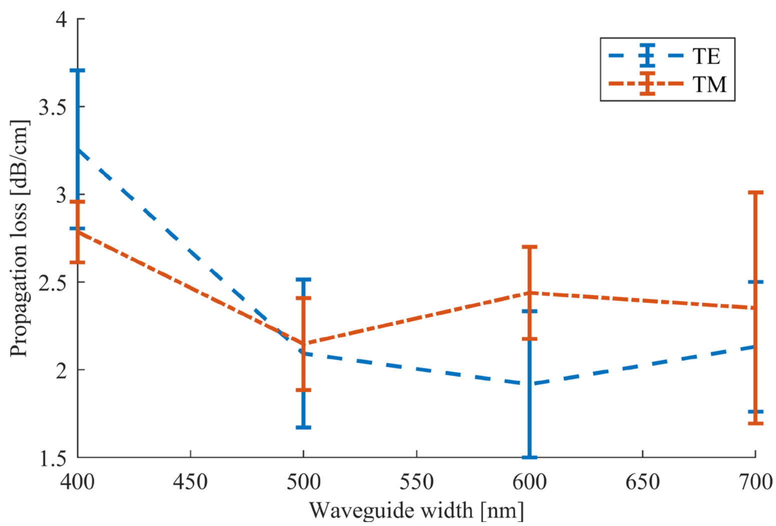

Figure 4 Propagation loss as a function of waveguide width for launched light of 405 nm. Error bars are the 95% confidence interval of the linear least squares fit.

4. CONCLUSION

We have demonstrated low-loss sputter coated Al_2O_3 waveguides with SiO_2 cladding, with losses down to 2 ± 0.5 dB/cm at 405 nm, comparable to the best results obtained with ALD deposited Al_2O_3. In addition the transmission bandgap down to 250 nm is verified showing the possibility for PICs in the UV.

REFERENCES

[1] W. Bogaerts *et al.*, "Programmable photonic circuits," *Nature*, vol. 586, no. 7828, pp. 207–216, Oct. 2020, doi: 10.1038/S41586-020-2764-0.

[2] H. Zia, N. M. Lüpken, T. Hellwig, C. Fallnich, and K. J. Boller, "Supercontinuum Generation in Media with Sign-Alternated Dispersion," *Laser Photonics Rev.*, vol. 14, no. 7, p. 2000031, Jul. 2020, doi: 10.1002/LPOR.202000031.

[3] C. Taballione *et al.*, "20-Mode Universal Quantum Photonic Processor," Mar. 2022, doi: 10.48550/arxiv.2203.01801.

[4] A. Leinse *et al.*, "TriPlex photonic platform technology: Low-loss waveguide platform for applications from UV to IR," *16th Eur. Conf. Integr. Opt.*, vol. 4, pp. 6–7, 2012.

[5] M. J. R. Heck *et al.*, "Ultra-low-loss high-aspect-ratio Si_3N_4 waveguides," *Opt. Express Vol 19 Issue 4 Pp 3163-3174*, vol. 19, no. 4, pp. 3163–3174, Feb. 2011, doi: 10.1364/OE.19.003163.

[6] T. J. Morin *et al.*, "CMOS-foundry-based blue and violet photonics," *Opt. Vol 8 Issue 5 Pp 755-756*, vol. 8, no. 5, pp. 755–756, May 2021, doi: 10.1364/OPTICA.426065.

[7] A. Siddharth *et al.*, "Near ultraviolet photonic integrated lasers based on silicon nitride," *APL Photonics*, vol. 7, no. 4, p. 046108, Apr. 2022, doi: 10.1063/5.0081660.

[8] M. Corato-Zanarella, A. Gil-Molina, X. Ji, M. C. Shin, A. Mohanty, and M. Lipson, "Widely tunable and narrow-linewidth chip-scale lasers from near-ultraviolet to near-infrared wavelengths," *Nat. Photonics*, pp. 1–8, Dec. 2022, doi: 10.1038/s41566-022-01120-w.

[9] K. R. Brown, J. Chiaverini, J. M. Sage, and H. Häffner, "Materials challenges for trapped-ion quantum computers", doi: 10.1038/s41578-021-00292-1.

[10] N. Hinkley *et al.*, "An Atomic Clock with 10–18 Instability," *Science*, vol. 341, no. 6151, pp. 1215–1218, Sep. 2013, doi: 10.1126/science.1240420.

[11] E. O. Filatova and A. S. Konashuk, "Interpretation of the Changing the Band Gap of Al2O3 Depending on Its Crystalline Form: Connection with Different Local Symmetries," *J. Phys. Chem. C*, vol. 119, no. 35, pp. 20755–20761, Aug. 2015, doi: 10.1021/acs.jpcc.5b06843.

[12] G. N. West *et al.*, "Low-loss integrated photonics for the blue and ultraviolet regime," *APL Photonics*, vol. 4, no. 2, p. 026101, Feb. 2019, doi: 10.1063/1.5052502.

[13] C. Lin *et al.*, "UV photonic integrated circuits for far-field structured illumination autofluorescence microscopy," *Nat. Commun. 2022 131*, vol. 13, no. 1, pp. 1–9, Jul. 2022, doi: 10.1038/s41467-022-31989-8.

[14] M. M. Aslan *et al.*, "Low-loss optical waveguides for the near ultra-violet and visible spectral regions with Al2O3 thin films from atomic layer deposition," *Thin Solid Films*, vol. 518, no. 17, pp. 4935–4940, Jun. 2010, doi: 10.1016/j.tsf.2010.03.011.